Gate-Controlled Spin-Valley Locking of Resident Carriers in WSe_{2} Monolayers

P. Dey, Luyi Yang, C. Robert, G. Wang, B. Urbaszek, X. Marie, and S. A. Crooker

Phys. Rev. Lett. **119**, 137401 — Published 27 September 2017

DOI: 10.1103/PhysRevLett.119.137401

Gate controlled spin-valley locking of resident carriers in WSe_2 monolayers

P. Dey[1], Luyi Yang[1], C. Robert[2], G. Wang[2], B. Urbaszek[2], X. Marie[2], S. A. Crooker[1]
[1] *National High Magnetic Field Laboratory, Los Alamos National Lab, Los Alamos, NM 87545, USA and*
[2] *Université de Toulouse, INSA-CNRS-UPS, LPCNO, 135 Av. Rangueil, 31077 Toulouse, France*

Using time-resolved Kerr rotation, we measure the spin/valley dynamics of resident electrons and holes in single charge-tunable monolayers of the archetypal transition-metal dichalcogenide (TMD) semiconductor WSe_2. In the n-type regime, we observe long (∼130 ns) polarization relaxation of electrons that is sensitive to in-plane magnetic fields B_y, indicating spin relaxation. In marked contrast, extraordinarily long (∼2 μs) polarization relaxation of holes is revealed in the p-type regime, that is unaffected by B_y, directly confirming long-standing expectations of strong spin-valley locking of holes in the valence band of monolayer TMDs. Supported by continuous-wave Kerr spectroscopy and Hanle measurements, these studies provide a unified picture of carrier polarization dynamics in monolayer TMDs, which can guide design principles for future valleytronic devices.

Besides their obvious promise for 2D optoelectronics [1–3], monolayer transition-metal dichalcogenide (TMD) semiconductors such as MoS_2 and WSe_2 have also revitalized interests in exploiting both the spin *and valley pseudospin* of electrons and holes for potential applications in (quantum) information processing [4–9]. This notion of "valleytronics" arises due to their crystalline asymmetry and strong spin-orbit coupling, which leads to spin-dependent band structure [10, 11], spin-valley locking, and valley-specific optical selection rules [7, 8]. These rules mandate that the K or K' valleys in momentum space can be selectively populated and probed using polarized light, in contrast with most conventional III-V, II-VI, and group-IV semiconductors. Therefore, information may be readily encoded not only by whether an electron (or hole) has spin "up" or "down", but *also* by whether it resides in the K or K' valley – or, indeed, in some quantum-mechanical superposition thereof.

The intrinsic timescales of carrier spin and valley dynamics in monolayer TMDs are therefore of considerable importance. However, most studies to date [12–18] have focused on photogenerated neutral and charged *excitons*, whose dynamics at low temperatures are inherently limited by their short (3-30 ps) recombination lifetimes [15, 19]. An essential but altogether different question, however, concerns the intrinsic spin/valley lifetimes of the *resident* electrons and holes that exist in n-type and p-type TMD monolayers. In future valleytronic devices, it is likely the properties of these resident carriers that will determine performance – analogous to how the scattering timecales and mobility of resident carriers (not excitons) determines the performance of modern-day transistors and interconnects.

Several recent time-resolved studies point to encouragingly long polarization dynamics of resident carriers in monolayer TMDs. 3-5 ns polarization decays were observed in CVD-grown MoS_2 and WS_2 monolayers that were unintentionally electron-doped [20, 21], while somewhat longer timescales were observed in unintentionally hole-doped CVD-grown WSe_2 [22, 23]. However, a significant shortcoming in all these studies is that the carrier densities were fixed and were due to uncontrolled background impurities. Therefore, systematic trends with doping density were impossible to identify. It is widely anticipated from theory, however, that spin/valley dynamics in TMD monolayers should depend sensitively on carrier density, particularly when tuning between n- and p-type regimes [7, 8]. This is because the huge valence band spin-orbit splitting requires that any $K \leftrightarrow K'$ valley scattering of holes must also flip spin (in contrast to the conduction band, where the spin-orbit splitting is much smaller), severely restricting available relaxation pathways [7]. Time-resolved studies of spin/valley dynamics, in which the carrier concentrations can be *systematically tuned* between n- and p-type in a single crystal, are therefore greatly desired, but have not been performed until now.

Here we experimentally demonstrate and directly validate long-standing predictions of exceptionally robust spin-valley polarization of resident holes in monolayer TMDs. Via time-resolved Kerr rotation studies of *charge-tunable* WSe_2 monolayers, we reveal the existence of extraordinarily longlived (2 μs) spin-valley polarization relaxation in the p-type regime. Much shorter polarization dynamics are observed for electrons in the n-type regime. Supported by continuous-wave Kerr spectroscopy and Hanle-effect studies, these measurements provide a unified picture of carrier polarization dynamics in the new family of monolayer TMD semiconductors.

Figure 1a depicts the experiment. Exfoliated WSe_2 monolayers were transferred onto split Cr/Au gate electrodes patterned on SiO_2/Si substrates. Structures with 80 and 300 nm SiO_2 were primarily used for static and time-resolved studies, respectively [24]. Compared to typical CVD-grown WSe_2, WS_2, or MoS_2, exfoliated WSe_2 exhibits much cleaner optical spectra. Of particular importance, and in contrast to earlier studies of resident carrier dynamics [20–23], the neutral (X^0) and charged exciton ($X^{\pm}$) transitions are spectrally resolved and can be probed separately. A gate voltage V_G tunes between n-type and p-type regimes, as confirmed in Figs. 1b,c by low-temperature reflection spectra. When nomi-

nally undoped (V_G=0), the spectra exhibit a single resonance at ∼712 nm corresponding to neutral "A" excitons, X^0. However when V_G>0 and the conduction bands fill with resident electrons, the X^0 resonance weakens and the negatively-charged exciton (X^-) resonance develops at ∼725 nm. The X^- is a three-particle complex consisting of a photogenerated electron-hole pair bound to an additional resident electron. Similarly, when V_G<0 and the valence bands fill with resident holes, the spectra evolve into the positively-charged exciton X^+ (an electron-hole pair bound to an additional resident hole) at ∼720 nm. This behavior agrees very well with past studies of gated WSe_2 monolayers [25].

The gated samples were studied using both continuous-wave and time-resolved Kerr rotation (CWKR, TRKR); Fig. 1a depicts the latter [24]. Right- or left-circularly polarized (RCP/LCP) pump pulses photoexcite excess spin-up or spin-down electrons and holes in the K or K' valley, respectively. At cryogenic temperatures, these photocarriers form excitons and trions that quickly scatter and recombine on short (<30 ps) timescales, as determined by time-resolved PL [15, 19]. In doing so they perturb the resident carriers away from thermal equilibrium, thereby transferring to them a non-zero spin/valley polarization. The mechanisms underpinning polarization transfer likely include exciton correlations and scattering while the photo-generated minority species are present [12–14, 18], and any non-radiative recombination of the minority species with resident carriers having opposing spin and/or valley. Related processes in conventional III-V and II-VI semiconductors are well-known to transfer spin polarizations to resident carriers in bulk, 2D, and 0D systems [26–31]. Regardless of the generation mechanism (which is not our focus), once the photoexcited carriers have recombined on short timescales, the spin/valley polarization of the resident carriers is *out of* equilibrium and will relax according to its intrinsic and much longer timescales. Our principal goal is to measure these fundamental intrinsic timescales in both electron- and hole-doped regimes, in the same TMD crystal.

The spin/valley polarization is monitored via the Kerr rotation θ_K imparted on time-delayed probe pulses from a tunable Ti:sapphire laser. An essential new aspect of this experiment is a fast electronic delay generator synchronized to an acousto-optic pulse-picker [24]. In contrast to prior TRKR studies [20–23], this combination enables pump-probe delays Δt up to *microseconds*, which greatly exceeds that of conventional optical delay lines, allowing direct access to the extremely long relaxation timescales that, we find, exist in monolayer WSe_2.

Figures 1d,e show the central result. In the heavily electron-doped regime, with the probe laser tuned near the X^- resonance, TRKR reveals surprisingly long polarization decays of ∼130 ns at 5 K. Crucially, these decays are suppressed in weak applied in-plane magnetic fields B_y<100 mT, strongly suggesting electron spin relaxation

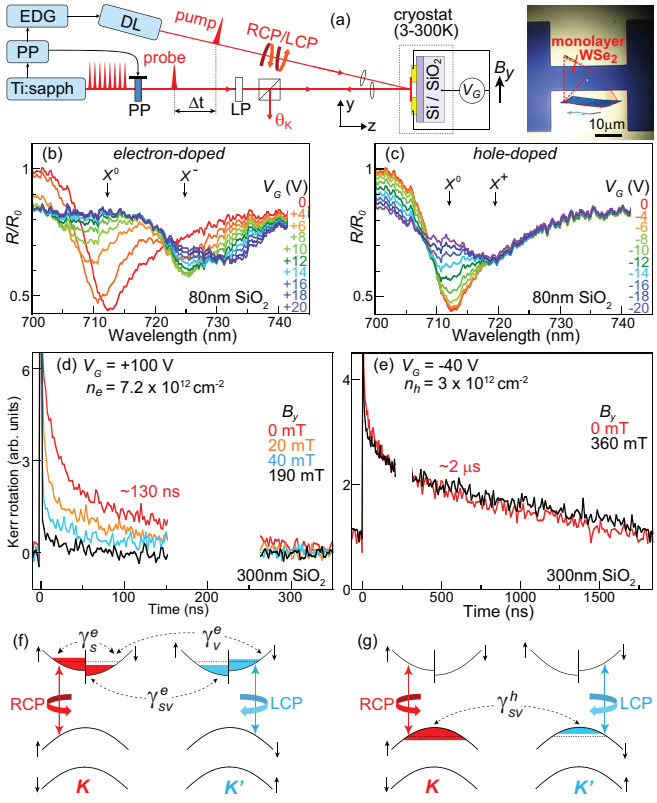

FIG. 1. (a) TRKR experiment on gated monolayer WSe_2. V_G tunes the resident carrier density between electron- and hole-doped regimes. External coils provide in-plane magnetic fields B_y. RCP or LCP pump pulses from a 645 nm diode laser (DL) imprint a spin/valley polarization on the resident carriers, which is detected via the Kerr rotation θ_K imparted on probe pulses from a Ti:S laser. A pulse-picker (PP) and electronic delay generator (EDG) allow access to μs pump-probe delays Δt. (b) Normalized reflection spectra R/R_0 versus V_G at 5 K (from 80 nm SiO_2 sample); the oscillator strength evolves from neutral exciton X^0 to negatively-charged exciton X^- with increasing electron density. (c) Similar evolution from X^0 to positively-charged exciton X^+ with increasing hole density. (d) TRKR in the heavily electron-doped regime at 5K (from 300 nm SiO_2 sample), with the probe tuned to 727 nm. For large Δt (>50 ns), the signal decays exponentially with ∼130 ns time constant. The decays are strongly suppressed in small B_y. (For technical reasons, Δt between 150-260 ns are not accessible [24]). (e) TRKR at 5K in the hole-doped regime at the X^+ transition: Extraordinarily long polarization decays are revealed (∼2 μs) that are *independent* of B_y, confirming strong spin-valley locking in the valence band. (f,g) The diagrams depict the simplest WSe_2 band structure in the electron and hole-doped regimes, along with available scattering pathways.

as the origin of this decay (discussed below). Most remarkably, however, when the same WSe_2 monolayer is populated with holes, TRKR studies with the probe at X^+ reveal extraordinarily long-lived polarization decays with a slow component of ∼2 μs. However, these slow decays are *not* affected by B_y, consistent with strong

spin-valley locking in the valence band.

To help understand these contrasting behaviors, Figs. 1f,g depict the simplest WSe_2 bandstructure and possible relaxation pathways. When the chemical potential μ ($\sim$34 meV in Fig 1d) exceeds the conduction band spin-orbit splitting, Δ_c ($\sim$25 meV in WSe_2 [32]), three pathways for resident electrons are identified: i) spin relaxation within a valley, given by rate γ_s^e, ii) spin-*conserving* intervalley scattering (γ_v^e), and iii) spin-*flip* intervalley scattering (γ_{sv}^e). The latter rate requires *both* spin and valley scattering, and is therefore likely small. In contrast, for resident holes the giant valence band spin-orbit splitting ($\Delta_v \sim 450$ meV) ensures that polarized holes can only relax by simultaneously scattering both spin *and* valley degrees of freedom. The corresponding rate, γ_{sv}^h, is therefore expected to be quite small [7, 8].

The markedly different dependence on B_y provides important information. In the n-type regime, the sensitivity to small B_y, and absence of any oscillatory TRKR signal, are consistent with the spin depolarization mechanism recently proposed for electron-doped MoS_2 [20], summarized here as follows: Δ_c is 'seen' by resident electrons as a *valley-dependent* effective spin-orbit field B_{so} oriented normal to the 2D plane (parallel to $\pm\hat{z}$, depending on whether the electron resides in K or K'). Being large (10s of tesla), B_{so} should stabilize an electron's spin along $\pm\hat{z}$, such that B_y has little effect. However, if spin-conserving $K \leftrightarrow K'$ scattering (γ_v^e) is fast (as believed for electrons when $\mu > \Delta_c$ [12, 33]), then B_{so} fluctuates rapidly between $\pm\hat{z}$. Therefore, the net field $B_y\hat{y} \pm B_{so}\hat{z}$ is both fluctuating *and* slightly canted, which will quickly depolarize electron spin, as experimentally observed. Within this model, the slow decay measured when B_y=0 is $1/\gamma_s^e$, the intravalley spin relaxation time (see Supplemental Material for details of the model, and also for measurements at elevated temperatures [24]).

In contrast, in the p-type regime Δ_v is huge, and spin-conserving intervalley scattering is suppressed as discussed above. B_{so} 'seen' by holes is gigantic ($>10^3$ T) and does not fluctuate. Hole spins are pinned along $+\hat{z}$ or $-\hat{z}$ and B_y should have little influence, as observed. The only available relaxation path is spin-flip valley scattering (γ_{sv}^h), measured to be $\sim$2 μs at 5 K. These results experimentally confirm the widely-believed theoretical prediction [7, 8] that spin-valley locking in the valence band leads to extremely robust spin-valley polarization of holes.

The remarkably stable hole polarizations in our WSe_2 monolayers are strongly supported by a recent report of microsecond hole polarizations of indirect excitons in WSe_2/MoS_2 *bilayers* [34]. Here, rapid electron-hole spatial separation following neutral exciton generation leads to long-lived indirect excitons, in which the electron and hole are very weakly bound and therefore depolarize essentially as independent particles, approximating the case of resident carriers. Our experiments on gated

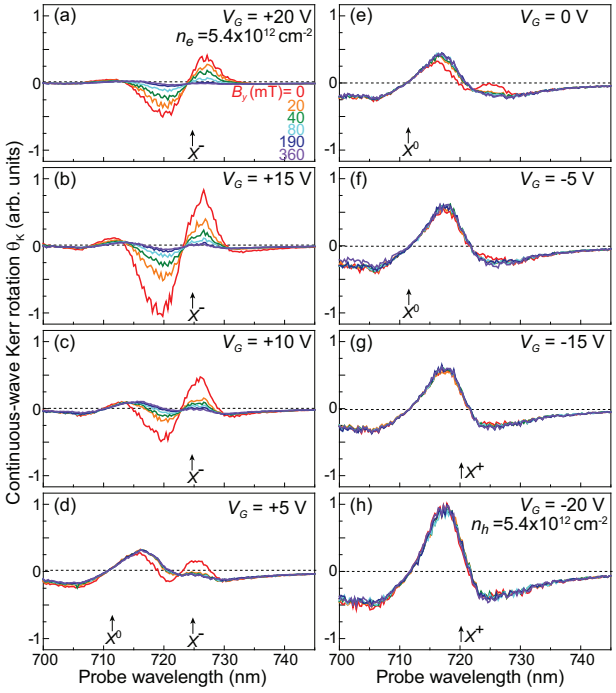

FIG. 2. (a-h) CWKR spectra at 5 K (from WSe_2 on 80 nm SiO_2) as the resident carrier density is tuned from the electron-doped to hole-doped. Within each panel, B_y is varied from 0 mT (red trace) to 360 mT (violet trace). The WSe_2 is weakly pumped by a circularly-polarized 632.8 nm CW laser, and the induced Kerr rotation is detected by a narrowband CW Ti:sapphire ring laser that is scanned from 700-750 nm. Positions of the neutral and charged exciton transitions from reflectivity studies of this sample (see Figs. 1b,c) are indicated.

WSe_2 monolayers directly confirm that resident holes indeed have intrinsically long polarization lifetimes due to spin-valley locking which is not limited by population decay. This suggests monolayer WSe_2 is an excellent building block for hole spin/valley storage in more complex van der Waals devices [2].

Moreover, the very different dynamics in n- and p-type regimes argues against these long decays being due to optically-forbidden ("dark") neutral excitons [32, 35], which likely exist in WSe_2 but which should exhibit similar dynamics in both regimes. We note, however, that putative *charged* dark excitons could in principle play a role in these gate-dependent studies [36].

Our TRKR results are supported by detailed CWKR spectroscopy, wherein a weak CW pump generates a *steady-state* non-equilibrium carrier polarization while a narrowband probe, scanned across the neutral and charged exciton transitions, detects θ_K [24]. Figure 2 shows CWKR spectra at various V_G spanning n- to p-type doping regimes. At each V_G, spectra are measured at different B_y (red to violet curves). When unambiguously electron-doped (Figs. 2a-c), the CWKR spectra exhibit a sizable Kerr resonance centered at $\sim$725 nm,

which corresponds to the X^- transition. The antisymmetric Kerr lineshape is typical, and reveals a large steady-state polarization. Consistent with TRKR studies, small B_y suppresses θ_K. We note that the largest signals are observed at V_G=+15 V, which corresponds in this sample to $\mu \sim \Delta_c \sim$25 meV. As $V_G \rightarrow 0$ and the electrons deplete, a smaller Kerr resonance develops at the X^0 transition (∼710 nm); however, it is largely unaffected by B_y, as expected [37].

Crucially, these data show that the resident carrier polarization appears to manifest itself primarily via the charged exciton transition. Analogous to the well-studied situation in III-V and II-VI semiconductors [28–31], this is likely because the probability for exciting a polarized X^- *necessarily* depends on the availability of appropriately-polarized resident electrons (or resident holes, for X^+ formation). Consider the simplest case of singlet X^-, wherein the photogenerated electron must have spin orientation opposite to the resident electron's. In the limit where the resident electrons are entirely polarized spin-up, the absorption of (say) RCP light at X^- will be entirely suppressed, while the absorption for LCP light remains large. This circular dichroism generates a large θ_K. Kerr rotation at the charged exciton transitions is therefore a sensitive probe of the resident carrier polarization. In contrast, X^0 formation does not depend explicitly on the polarization of a third (resident) particle. This further highlights the importance of using exfoliated WSe_2: resolving the very different trends at X^0 and X^- provides essential insight into the underlying mechanisms. In many recent TRKR studies of CVD-grown MoS_2, WS_2, and WSe_2 [20–23], a clear separation between neutral and charged excitons was not possible.

Returning to Fig. 2, when the WSe_2 is p-type the CWKR spectrum distorts, grows, and develops a sharp zero-crossing at ∼720 nm, which corresponds to the X^+ transition. Consistent with the TRKR data, these large CW Kerr signals reflect a buildup of steady-state hole polarization, and – importantly – are *not* influenced by B_y due to spin-valley locking.

Finally, we perform Hanle effect measurements (*i.e.*, carrier depolarization by B_y), which have historically played a central role in semiconductor spintronics [26, 27] to determine spin lifetimes, nuclear fields, and spin-orbit effects. Figure 3 shows θ_K versus B_y as the WSe_2 monolayer is tuned from n- to p-type. When probing at 727 nm – where both X^- and X^+ give appreciable θ_K – the signals in the electron-doped regime exhibit narrow peaks indicating that small B_y dephases the electron polarization (as known from TRKR studies). The peak widths are narrowest (18 mT) when lightly electron-doped, but increase to >60 mT at higher electron densities. However, as discussed in [20], the Hanle width in monolayer TMDs does not simply reflect the spin relaxation rate (as in conventional semiconductors), but rather equals $\gamma_s^e\sqrt{1+\Omega_{so}^2/2\gamma_s^e\gamma_v^e}$, where Ω_{so} is the spin precession frequency due to B_{so}. The observed trend is consistent with increased total spin-orbit splitting 'seen' by electrons as μ increases, because the spin-up and spin-down bands are not only split by Δ_c but also have different curvatures. Conversely, in the hole-doped regime the traces are flat because B_y does not affect the hole polarization due to spin-valley locking. Further, Fig. 3b shows Hanle studies at the X^0 resonance (706 nm). Here, θ_K is essentially unaffected by B_y for *all* V_G, again indicating that X^0 is uninfluenced by the resident carrier polarization.

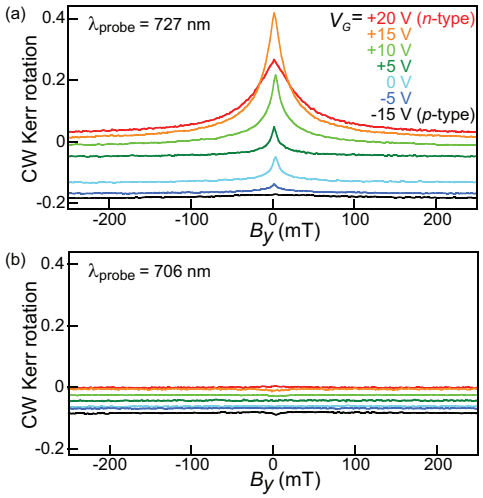

FIG. 3. (a) Hanle-Kerr effect as the WSe_2 monolayer is tuned from n-type to p-type regime (in the 80 nm SiO_2 structure). The WSe_2 is weakly pumped by a circularly-polarized 632.8 nm CW laser. B_y is continuously varied while the induced Kerr rotation is measured by a tunable CW probe laser. Here the probe is fixed at 727 nm, which is sensitive to both X^- and X^+ transitions. The width of the Hanle curves increases with increasing electron density in the n-type regime. In the p-type regime the Hanle curves show no dependence on B_y. (b) Same, but the probe laser is fixed at 706 nm, which is sensitive to the neutral X^0 exciton transition. No dependence on B_y observed.

Taken all together, these time-resolved and steady-state Kerr studies of single gated TMD monolayers significantly advance a unified picture of spin and valley dynamics of resident carriers in atomically-thin semiconductors. Controlling strong spin-valley locking and ultralong polarization storage lifetimes by tuning between n- and p-type doping will likely be significant for future TMD-based valleytronics using van der Waals devices.

P.D., L.Y., and S.A.C. gratefully acknowledge support from the Los Alamos LDRD program and the NHMFL, which is supported by NSF DMR-1157490. C.R. and X.M. thank ANR MoS_2ValleyControl, G.W. and B.U. thank ERC Grant No. 306719; X.M. also acknowledges the Institut Universitaire de France. We also thank M. Pierre, W. Escoffier and B. Lassagne for device fabrication help, and S. Tongay for the growth of bulk WSe_2.

[1] Q. H. Wang, K. Kalantar-Zadeh, A. Kis, J. N. Coleman, and M. S. Strano, Nat. Nanotechnol. **7**, 699 (2012).
[2] A. K. Geim and I. V. Grigorieva, Nature **499**, 419 (2013).
[3] K. F. Mak and J. Shan, Nat. Photon. **10**, 216 (2016).
[4] O. Gunawan, Y. P. Shkolnikov, K. Vakili, T. Gokmen, E. P. De Poortere, and M. Shayegan, Phys. Rev. Lett. **97**, 186404 (2006).
[5] D. Xiao, W. Yao, and Q. Niu, Phys. Rev. Lett. **99**, 236809 (2007).
[6] A. Rycerz, J. Tworzydło, and C. W. J. Beenakker, Nat. Phys. **3**, 172 (2007).
[7] D. Xiao, G. B. Liu, W. X. Feng, X. Xu, and W. Yao, Phys. Rev. Lett. **108**, 196802 (2012).
[8] X. Xu, W. Yao , D. Xiao, and T. F. Heinz, Nat. Phys. **10**, 343 (2014).
[9] K. F. Mak, K. L. McGill, J. Park, and P. L. McEuen, Science **344**, 1489 (2014).
[10] J. M. Riley, F. Mazzola, M. Dendzik, M. Michiardi, T. Takayama, L. Bawden, C. Granerød, M. Leandersson, T. Balasubramanian, M. Hoesch, T. K. Kim, H. Takagi, W. Meevasana, Ph. Hofmann, M. S. Bahramy, J. W. Wells, and P. D. C. King, Nat. Phys. **10**, 835 (2014).
[11] Y. Zhang, M. M. Ugeda, C. Jin, S.-F Shi, A. J. Bradley, A. Martín-Recio, H. Ryu, J. Kim, S. Tang, Y. Kim, B. Zhou, C. Hwang, Y. Chen, F. Wang, M. F. Crommie, Z. Hussain, Z.-X Shen, and S.-K. Mo, Nano Lett. **16**, 2485 (2016).
[12] C. Mai, A. Barrette, Y. Yu, Y. G. Semenov, K. W. Kim, L. Cao, and K. Gundogdu, Nano Lett. **14**, 202 (2014).
[13] A. Singh, G. Moody, S. Wu, Y. Wu, N. J. Ghimire, J. Yan, D. G. Mandrus, X. Xu, and X. Li, Phys. Rev. Lett. **112**, 216804 (2014).
[14] T. Yu and M. W. Wu, Phys. Rev. B **89**, 205303 (2014).
[15] G. Wang, L. Bouet, D. Lagarde, M. Vidal, A. Balocchi, T. Amand, X. Marie, and B. Urbaszek, Phys. Rev. B **90**, 075413 (2014).
[16] C. R. Zhu, K. Zhang, M. Glazov, B. Urbaszek, T. Amand, Z. W. Ji, B. L. Liu, and X. Marie, Phys. Rev. B **90**, 161302(R) (2014).
[17] K. Hao, G. Moody, F. Wu,C. K. Dass, L. Xu, C.-H. Chen, L. Sun, M.-Y. Li, L.-J. Li, A. H. MacDonald, and X. Li, Nat. Phys. **12**, 677 (2016).
[18] R. Schmidt, G. Berghauser, R. Schneider, M. Selig, P. Tonndorf, E. Malic, A. Knorr, S. M. de Vasconcellos, and R. Bratschitsch, Nano Lett. **16**, 2945 (2016).
[19] C. Robert, D. Lagarde, F. Cadiz, G. Wang, B. Lassagne, T. Amand, A. Balocchi, P. Renucci, S. Tongay, B. Urbaszek, and X. Marie, Phys. Rev. B **93**, 205423 (2016).
[20] L. Yang, N. A. Sinitsyn, W. Chen, J. Yuan, J. Zhang, J. Lou, and S. A. Crooker, Nat. Phys. **11**, 830 (2015).
[21] E. J. Bushong, Y. Luo, K. M. McCreary, M. J. Newburger, S. Singh, B. T. Jonker, and R. K. Kawakami, Preprint at arXiv:1602.03568 (2016).
[22] W.-T. Hsu, Y.-L. Chen, C.-H. Chen, P.-S. Liu, T.-H. Hou, L. J. Li, and W.-H. Chang, Nat. Commun. **6**:8963 (2015).
[23] X. Song, S. Xie, K. Kang, J. Park, and V. Sih, Nano Lett. **16**, 5010 (2016).
[24] See Supplemental Material [url] for experimental details and supporting data, which includes Refs [38-42].
[25] A. M. Jones, H. Yu, N. J. Ghimire, S. Wu, G. Aivazian, J. S. Ross, B. Zhao, J. Yan, D. G. Mandrus, D. Xiao, W. Yao, and X. Xu, Nat. Nanotech. **8**, 634 (2013).
[26] R. I. Dzhioev, K. V. Kavokin, V. L. Korenev, M. V. Lazarev, B. Ya. Meltser, M. N. Stepanova, B. P. Zakharchenya, D. Gammon, and D. S. Katzer, Phys. Rev. B **66**, 245204 (2002).
[27] M. Furis, D. L. Smith, S. Kos, E. S. Garlid, K. S. M. Reddy, C. J. Palmstrøm, P. A. Crowell, and S. A. Crooker, New J. Phys. **9**, 347 (2009).
[28] D. R. Yakovlev and M. Bayer, Chapter 6, Spin Physics in Semiconductors, M. I. Dyakonov, editor (Springer, Berlin 2008).
[29] Z. Chen, S. G. Carter, R. Bratschitsch, and S. T. Cundiff, Physica E **42**, 1803 (2010).
[30] M. Atatüre, J. Dreiser, A. Badolato, A. Högele, K. Karrai, and A. Imamoglu, Science **312**, 551 (2006).
[31] A. Greilich, D. R. Yakovlev, A. Shabaev, Al. L. Efros, R. Oulton, V. Stavarache, D. Reuter, A. Wieck, and M. Bayer, Science **313**, 341 (2006).
[32] X. X. Zhang, T. Cao, Z. Lu, Y.-C. Lin, F. Zhang, Y. Wang, Z. Li, J. C. Hone, J. A. Robinson, D. Smirnov, S. G. Louie, and T. F. Heinz, Nat. Nanotechnol. Article Online doi:10.1038/nnano.2017.105
[33] B. Radisavljevic and A. Kis, Nat. Mater. **12**, 815 (2013).
[34] J. Kim, C. Jin, B. Chen, H. Cai, T. Zhao, P. Lee, S. Kahn, K. Watanabe, T. Taniguchi, S. Tongay, M. F. Crommie, and F. Wang, Sci. Adv. **3**, e1700518 (2017)
[35] G. Plechinger, P. Nagler, A. Arora, R. Schmidt, A. Chernikov, A. Granados del Aguila, P.C.M. Christianen, R. Bratschitsch, C. Schüller, and T. Korn, Nat. Commun. **7**:12715 (2016).
[36] F. Volmer, S. Pissinger, M. Ersfeld, S. Kuhlen, C. Stampfer, and B. Beschoten, Phys. Rev. B **95**, 235408 (2017).
[37] G. Sallen, L. Bouet, X. Marie, G. Wang, C. R. Zhu, W. P. Han, Y. Lu, P. H. Tan, T. Amand, B. L. Liu, and B. Urbaszek, Phys. Rev. B **86**, 081301(R) (2012).
[38] J. Dreiser, M. Atatüre, C. Galland, T. Müller, A. Badolato, and A. Imamoglu, Phys. Rev. B **77**, 075317 (2008).
[39] Y. Song and H. Dery, Phys. Rev. Lett. **111**, 026601 (2013).
[40] T. Uenoyama and L. J. Sham, Phys. Rev. B **42**, 7114 (1990).
[41] A. Kormányos, G. Burkard, M. Gmitra, J. Fabian, V. Zólyomi, N. D. Drummond, and V. Fal'ko, 2D Materials **2**, 022001 (2015).
[42] A. O. Slobodeniuk and D. M. Basko, 2D Materials **3**, 035009 (2016).